LBL-15017
Preprint c.2

Lawrence Berkeley Laboratory

UNIVERSITY OF CALIFORNIA

RECEIVED
LAWRENCE
BERKELEY LABORATORY
DEC 7 1982
LIBRARY AND
DOCUMENTS SECTION

Materials & Molecular Research Division

Submitted to WEAR

METHODS FOR CHARACTERIZATION OF EROSION BY GAS-ENTRAINED SOLID PARTICLES

Jennifer K. Patterson and Alan V. Levy

August 1982

TWO-WEEK LOAN COPY

This is a Library Circulating Copy which may be borrowed for two weeks. For a personal retention copy, call Tech. Info. Division, Ext. 6782.

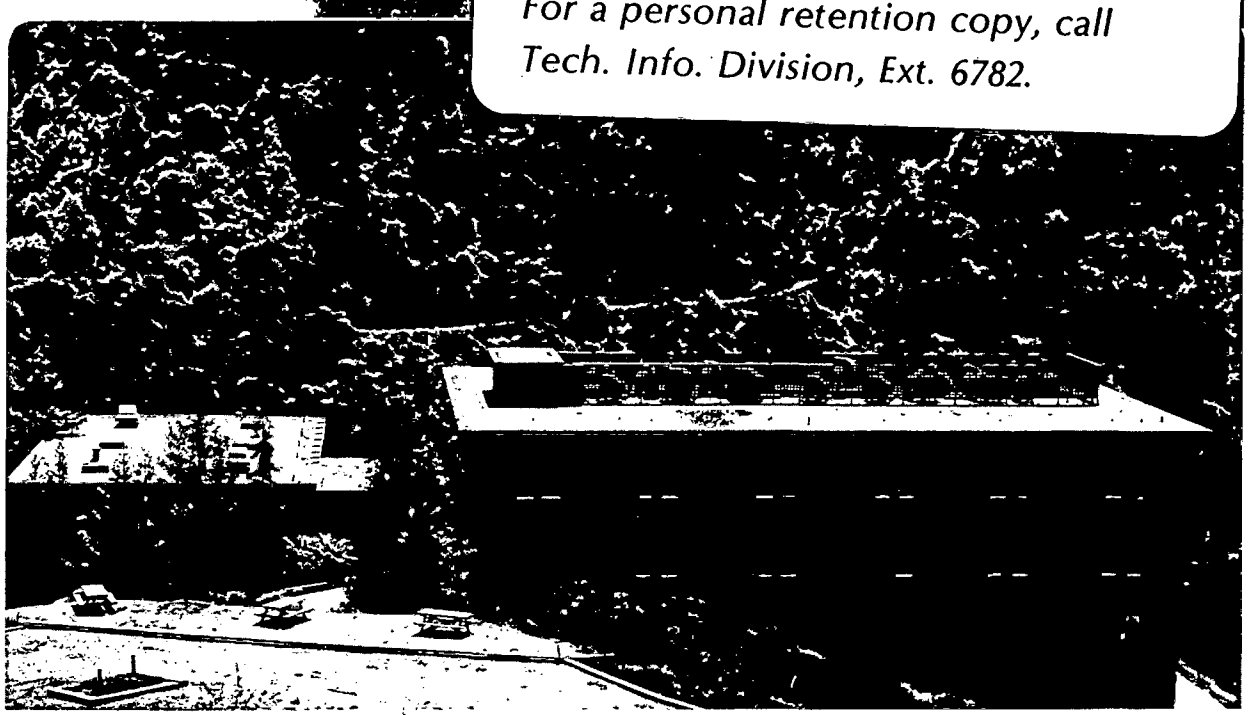

LBL-15017 c.2

Prepared for the U.S. Department of Energy under Contract DE-AC03-76SF00098

DISCLAIMER

This document was prepared as an account of work sponsored by the United States Government. While this document is believed to contain correct information, neither the United States Government nor any agency thereof, nor the Regents of the University of California, nor any of their employees, makes any warranty, express or implied, or assumes any legal responsibility for the accuracy, completeness, or usefulness of any information, apparatus, product, or process disclosed, or represents that its use would not infringe privately owned rights. Reference herein to any specific commercial product, process, or service by its trade name, trademark, manufacturer, or otherwise, does not necessarily constitute or imply its endorsement, recommendation, or favoring by the United States Government or any agency thereof, or the Regents of the University of California. The views and opinions of authors expressed herein do not necessarily state or reflect those of the United States Government or any agency thereof or the Regents of the University of California.

LBL-15017

Methods for Characterization of Erosion by Gas-Entrained Solid Particles

Jennifer K. Patterson and Alan V. Levy

Materials and Molecular Research Division
Lawrence Berkeley Laboratory
University of California
Berkeley, California 94720

Research sponsored by the Department of Energy under DOE/FEAA 15 10 10 0, Advanced Research and Technical Development, Fossil Energy Materials Program, Work Breakdown Structure Element LBL-3.5 and under Contract No. DE-AC03-76SF00098.

LBL-15017

METHODS FOR CHARACTERIZATION OF EROSION BY GAS-ENTRAINED SOLID PARTICLES

JENNIFER K. PATTERSON and ALAN V. LEVY

Materials and Molecular Research Division, Lawrence Berkeley Laboratory,

University of California, Berkeley, California 94720

Summary

Criteria for the preparation of metal specimens used in solid-gas erosion testing are presented. The equipment and methods of erosion testing are described, and methods for measurement of solid particle velocity are reviewed. An experimental technique based on time-series analysis is proposed. The effect of sample preparation and data analysis methods on reproducibility and scattering of measured erosion rates is presented. A method for reducing errors in erosion rates is suggested.

---

1. Introduction

The degradation of materials by solid particle erosion is responsible for equipment losses valued in the millions of dollars annually. The problem is widespread in the chemical process industries and in equipment used in dusty and sandy environments. Particle erosion can accelerate the rate of chemical corrosion processes. Material degradation in the combined erosion-corrosion process occurs at a rate significantly more rapid than either single process, and may even limit the application of

Research sponsored by the Department of Energy under DOE/FEAA 15 10 10 0, Advanced Research and Technical Development, Fossil Energy Materials Program, Work Breakdown Structure Element LBL-3.5 and under Contract No. DE-AC03-76SF00098.

coal conversion systems. Controlled studies of erosion are conducted to provide an understanding of erosion and of the coupled phenomenon.

The study of gas-solid particle erosion has received much attention since the 1960's [1-5]. The purpose of this work is to present the methods used in the experimental study of erosion of ductile metals. Sample preparation, erosion testing, data analysis, and the characteristic errors that can occur are discussed.

2. Sample preparation

The preparation of erosion test specimens consists of cutting or shearing the test specimen to the appropriate size and removing deformed surface layers by grinding and polishing.

2.1. Cutting and shearing

Two methods have been used for sizing erosion test specimens: cutting with a band saw, and shearing with a metal shear. Shearing has the advantage of producing specimens quickly. The sheared specimen is compressed and bent inward resulting in the permanently deformed specimen illustrated in Figure 1. The representative flat surface area available for testing is reduced substantially; the amount of area reduction varies with the ductility of the metal. A soft, 3/4-inch square 1100-0 aluminum sample, for example, loses about 50 percent of its available test area through shearing, thereby requiring a larger specimen. The size of the erosion test specimen should be minimized in order to minimize the difference between the orders of magnitude of the sample weight (10 to 30 gm) and its erosive weight loss (0.0001 to 0.010 gm). Cutting is therefore the preferred technique for sizing ductile erosion test specimens that are subject to gravimetric analysis. Shearing is an adequate method for specimens to be examined by microscopy as long as the specimen provides an undeformed area of sufficient size for testing.

2.2. Grinding and polishing

The removal of deformed surface layers and the creation of a smooth, flat surface are accomplished by grinding and polishing. Standard references are available for specific information and techniques (see, e.g., Petzow [6]). Generally, grinding results in a surface roughness between 1

and 100 μm, and polishing results in a sub-micron, mirror-like finish.

Most erosion test specimens are cut from sheet metal that has been rolled to final thickness. The rolling process deforms surface layers to a depth that varies depending upon the type of metal, but is in the order of tens of microns [7]. Removal of these deformed layers, using standard metallographic techniques, allows erosion to begin on a surface that is characteristic of the bulk. The final degree of roughness is determined by the test objectives. Polishing, for example, is not needed for a metal specimen tested under very erosive conditions. Polishing is needed to achieve reproducibility in single particle impact tests. A summary of specimen preparation guidelines is presented in Table 1 for various tests. The erosion severity of the test depends upon particle size, angularity, and hardness, test material hardness, particle velocity, and the distance between the nozzle and the specimen. The degree of surface roughness that is acceptable for an experiment can be determined by examining the effect of surface preparation. The criterion is that the amount of erodent required to remove surface deformation be small compared to the total weight of erodent used in the test.

A unique problem arises in the preparation of some very soft metals such as 1100-0 aluminum. Abrasive particles, not visible to the naked eye, are embedded in the specimen surface during grinding and polishing. Erosion testing of this uncharacteristic surface can result in misleading results. Electrolytic polishing is recommended for such materials [6].

3. Erosion testing

Typical erosion testing equipment resembles, in concept, a sand blaster. Erodent particles are propelled through a nozzle and strike the specimen surface. The eroded specimen is then analyzed. Gravimetric techniques are used to obtain erosion rates, and electron microscopy is used to reveal surface effects.

3.1. Equipment

A schematic diagram of a room temperature erosion tester [8] is shown in Figure 2. Erodent particles are placed in the hopper. An air-powered vibrator initiates flow of particles into the nozzle.

The particles are entrained in the carrier gas, carried through the nozzle and into the specimen chamber where they impinge upon the specimen surface.

The particle velocity, the distance between the nozzle and the specimen surface, and the angle of particle impingement are the test parameters that can be varied with this design. The particle velocity is a function of the nozzle diameter and its surface roughness, the pressure drop across the nozzle, the loading factor, and the size and shape of the erodent particles.

The loading factor is the ratio between the gas and particle mass flow rates. The loading factor is controlled by the angle of hopper inclination (expressed as Δ in Figure 2) and the vibrator air pressure. The particle and carrier gas velocities are controlled by varying the pressure drop across the nozzle. The vibrator air pressure is generally fixed, and the relative magnitudes of the hopper angle and the pressure drop are determined experimentally [9]. The approximate range of particle sizes that can be used in this tester is between 25 μm and 5 mm. The upper limit is determined by nozzle diameter restrictions. The lower limit is based upon the tendency of very fine, light particles to pack together rather than flow when vibration is applied to the hopper.

Pressure drops between 0 and 2 psi are read from an expanded scale manometer, and pressure drops above 2 psi are read from a standard pressure gauge. Routine calibration is performed to ensure accurate measurement of this parameter.

Sources of error that can be attributed to the test equipment include variation in the particle flow rate and malfunction of the pressure gauge or manometer. A variation in the particle flow rate is inherent in the use of the vibratory feed mechanism when used to deliver an aliquot of erodent particles. The particle mass flow rate is presented in Figure 3 as a function of diminishing erodent weight in the hopper. The standard deviation in flow rate from the average is 16 percent. A screw-type particle feed mechanism yields a constant flow rate, but severe maintenance problems can be associated with a feed mechanism in which moving parts are exposed to erodent particles. A change in the particle mass flow rate affects the particle velocity. Performing the velocity tests with the same amount of erodent as is to be used for the particular erosion test yields the "average" velocity and is probably the preferred method of minimizing this source of inaccuracy for most applications.

A second category of equipment-introduced inaccuracy can be avoided with routine maintenance and proper use of the equipment. Extended use of the equipment will eventually result in erosion of the nozzle by erodent particles. Changes in the nozzle diameter and roughness by erosion of the nozzle produces a different velocity than that obtained with a new nozzle. The nozzle should therefore be routinely changed. A large angle of inclination of the hopper can increase the particle flow rate to a level too high for uniform entrainment in the air stream at the given air flow rate and cause "flooding" of the nozzle. A severe oscillation of the pressure drop across the nozzle is induced. When this effect is observed with the pressure gauge, the hopper angle should be reduced.

The functionality between erosion rates and the specimen-nozzle distance has not been determined, however the erosion rate is known to be highly sensitive to even slight changes in this distance. It is essential that all specimens be compared on the same basis. A working distance of 0.5 inch is a good standard measurement.

3.2. Velocity measurement

The measurement of solid particle velocities is essential for the characterization of gas-solid particle erosion. The erosion rate of ductile metals is proportional to the second to third power of erodent particle velocity. A 20 percent uncertainty in velocity results in a 40 percent uncertainty in the erosion rate. Accurate measurement of this parameter is difficult. The techniques that have been used are multiple flash photography, the high speed cine-camera, the streaking camera, the double rotating disk, and the laser doppler velocimeter. These techniques have been reviewed recently [10]. An experimental method that uses time-series analysis is presented.

Multiple flash photography involves identifying a particle in two different positions on a double exposed photograph. The time interval between the two exposures is known, and thus presents a means of calculating the particle velocity. The technique is relatively simple and is best used for single particle impact studies with a particle size above 25 μm. It has an uncertainty of 10 percent [10]. The high speed cine-camera technique is similar to multi-flash photography, except that single exposures of consecutive films are made instead of multiple exposures on the same film. The same particle constraints exist and the same order of uncertainty [10]. The streaking camera

technique uses a rotating arm camera and a lens-mirror system to capture particle images as they pass across the film. Again, particles must be above 25 μm in diameter. The uncertainty in the velocity measurement is 7 percent. The technique has the advantage over the other photographic techniques of being applicable to systems using a higher particle density [10]. The photographic techniques are limited to single particle impacts with particles above 25 μm in diameter. In a multi particle stream, a large measure of uncertainty exists in ascertaining that the particle identified in the second exposure was the same one identified in the first.

The double rotating disk method was developed by the National Bureau of Standards [11]. As shown in Figure 4, it consists of two disks rotating on a common shaft. Erodent particles are propelled from a nozzle through a radial slit of the upper disk. They then impinge on the lower disk where a small mark in eroded. The displacement of this spot from a line normal to slit on the upper disk is dependent upon the angular velocity of the disks and the particle velocity. The double rotating disk method is economical and easy to use. It cannot be used for single particle impacts. The rotation of the disks disturbs the particle flow field and results in an uncertainty of about 20 percent.

The laser doppler velocimeter consists of a laser beam that is split into two beams of equal intensity. An optical transmitter focuses the beams so that they intersect each other forming what is called the measuring volume. A particle passing through the measuring volume scatters light with a frequency that is proportional to its velocity. The measurement is based upon the average of several thousand particles and has typical uncertainties of 3 percent [10]. The laser doppler velocimeter can be used with particles ranging in size between 0.5 and 500 μm. It produces very reliable results but has the disadvantages of very high capital costs and applicability to limited particle flow densities.

The flow of erodent particles from the nozzle is inherently stochastic in nature. A method for measurement of solid particle velocities in stochastic gas-solid flow fields has been presented by Oki et al. [12]. A fiber optic probe, shown in Figure 5, is inserted in or near the flow field. Light from a laser shines into the field through a central tube. A particle moving downward reflects light, first

into the upper tube and then into the lower tube. Photovoltaic cells convert the light signal into electrical signals. These signals are compared using time-series techniques [13-15].

The signals from the upper and lower tubes (see Figure 5) are related by a time constant which represents the time of travel for a particle moving between the upper and lower tubes. This distance between the tubes can be measured, therefore the velocity can be calculated. The methods of analysis are presented elsewhere [13-15].

The time-series analysis method of measuring particle velocity yields a local velocity averaged over the time of measurement. The accuracy of the measurement is limited by the accuracy of the measurement of the particle path length. While the optical probe appears appropriate for this system, other methods of generating signals can also be used [15]. Further study is recommended to confirm the applicability of this method to erosion testing.

A computer model was developed by C.T. Crowe [16] and extended by D.M. Kleist [16] which predicted the velocity of solid particles entrained in a gas stream. The model is based upon mass, momentum, and energy conservation of each phase as well as momentum and energy transfer between phases. The transfer equations incorporate the equation of state, convective heat transfer between particles and gas, wall friction, particle-gas mass flow ratio, particle trajectory, aerodynamic drag on the particle due to its relative motion with respect to the gas and other parameters such as particle size and density, local pressure and temperature. The theoretical predictions of this program deviate from experimentally determined velocity measurements (using the rotary disk method) by $+8$ percent to -4 percent with an average of ± 3 percent depending upon particle characteristics such as size and shape. This model is sometimes used as an alternative to particle velocity measurement. The computer method is approximately comparable in uncertainty to the rotary disk velocity determination. The model has the advantage of being applicable to the high particle loading factors and for high temperatures as well as room temperature applications.

3.3. Method of erosion testing

Various types of erosion tests are performed, but the testing method remains basicly the same. The specimen is exposed to a known weight of erodent, cleaned, weighed, and analyzed.

Single particle impact studies involve the bombardment of the test sample with a few (5-10) individual particles, with subsequent examination of the impact sites.

In steady state erosion studies, the specimen is subjected to repeated blasts of a given weight of erodent, typically in the order of 30 grams, with the sum of the increments in the hundreds of grams. Between blasts, the specimen is cleaned and weighed. Other tests involve a single sustained blast of a few hundred grams of erodent particles. The objective of most gravimetric analysis is to obtain an erosion rate. The erosion rate is one of the most widely used parameters in the study of erosion, and is subject to characteristic errors.

The typical procedure for measuring incremental erosion rates consists of:

1. characterization of the metal surface
2. erosion of the surface with an increment of erodent
3. cleaning of the metal surface
4. weighing of the sample
5. reintroduction of the sample into the erosion chamber for further erosion.

The method used to clean the sample before weighing is critical to the accurate measurement of erosion rates. Two methods are compared here: wiping with a tissue and ultrasonic cleaning in alcohol. The specimen weight is presented in Figure 6 as a function of the erodent weight for a 304 stainless steel specimen that was tissue cleaned between blasts. The results of the identical experiment conducted with the specimen ultrasonically cleaned between blasts is presented in the same figure. The ultrasonically-cleaned specimen was eroded at a rate of 0.0001800 (gm sample)/(gm erodent) while the tissue-cleaned specimen was eroded at a rate of 0.0001125 (gm sample)/(gm erodent). Erodent particles, dust, and eroded metal dust adhered to the tissue-cleaned metal surface, causing a 38 percent decrease in the erosion rate. The erodent particles were attacking a metal surface that was mechanically protected, and the effect of particle impact and the erosion rate was reduced. Complete removal of loose material from the sample by ultrasonic cleaning allows accurate measurement of erosion rates.

Embedding of erodent particles arises with the erosion of some soft metals such as aluminum and lead, and of harder metals at higher temperatures at which they become soft. This phenomenon may be difficult to detect because it is not always manifested as a weight gain, yet it produces severe alteration of the surface structure. Embedded erodent particles can be detected by Kevex or Auger spectroscopy. Though no means of eliminating the problem has been found, it has been circumvented by using spherical erodents which do not easily embed [17,18].

Kosel [19] obtained erosive weight change data by the dissolution of nickel specimens in acid and weighing the insoluble alumina erodent. An unsuccessful attempt was made in this group to determine the true erosive weight loss by dissolving an aluminum specimen in hydrochloric acid and weighing the insoluble silicon carbide. Unfortunately, the aluminum did not dissolve completely. Because the severe alteration of the specimen surface precluded measurement of the true erosive weight loss in any case, the dissolution technique has not been pursued. The study of the erosion of soft metals is typically carried out with spherical erodents or with the presence of embedded particles reported with the results.

4. Data analysis

The gravimetric data obtained from erosion studies are typically used to obtain an erosion rate that represents the mass of erosive material loss as a function of the mass of impinging erodent particles. The measurement of the sample weight as a function of the mass of erodent is used to obtain the rate of erosion.

The erosion rate is the time derivative of the sample weight with respect to the mass of erodent striking the sample;

$$\frac{dm_s}{dt} = q_e \frac{dm_s}{dm_e} \tag{1}$$

where q_e is the mass flux of erodent, m_s is the mass of the sample, and m_e is the mass of the erodent. The derivative with respect to the erodent mass is the quantity usually reported.

Two methods may be used to obtain this derivative. The first involves the use of a finite difference approximation such as:

$$\left(\frac{dm_s}{dm_e}\right)_{m_{e_2}} \sim \frac{m_{s_2} - m_{s_1}}{m_{e_2} - m_{e_1}} \tag{2}$$

where m_{s_1} and m_{e_1} are the masses of the sample and the erodent evaluated at time 1 and m_{s_2} and m_{e_2} are the masses of the sample and the erodent evaluated at time 2. Since $(m_{e_2} - m_{e_1})$ is frequently a constant, some investigators use the finite difference approximation by reporting a weight loss, $(m_{s_2} - m_{s_1})$.

The finite-difference approximation is poor when $(m_{e_2} - m_{e_1})$ is large, and is increasingly valid as $(m_{e_2} - m_{e_1})$ approaches zero. As the incremental erodent weight becomes small, however, the change in the sample weight also becomes small. In this range, the finite difference approximation becomes limited by round-off errors.

Round-off errors occur as the result of subtracting two numbers that are very close to the same value. With the use of precision balances, the value of each weight can be obtained to six or seven significant figures. The difference of these two numbers, however, may have but one significant figure.

The magnitude of the error due to round-off is obtained using the total derivative;

$$\Delta E = \frac{\Delta m_s}{(m_{e_2} - m_{e_1})} + \frac{(m_{s_2} - m_{s_1})}{(m_{e_2} - m_{e_1})^2}\,\Delta m_e \tag{3}$$

where ΔE is the total error in the calculated erosion rate $\frac{dm_s}{dm_e}$, Δm_e is the error in the erodent mass, and Δm_s is the error in the sample mass. An error represented by equation (3) can easily be of the same magnitude as the rate itself. The finite difference method is limited, therefore, by finite difference errors with large incremental erodent weights and by round-off errors when the incremental erodent weight is small.

A superior approach for obtaining accurate erosion rate measurements uses all the data to get a least squares or visual fit relationship for the raw data. This curve can subsequently be analytically or graphically differentiated. The advantage of this method is that the scatter in the erosion rates introduced by round-off errors is avoided.

A comparison of the erosion rates obtained by the two methods is presented in Figures 7 and 8. These data represent weight losses in the 0.1 milligram range, and are therefore subject to serious round-off error. The data points in Figure 7 are so widely scattered as to make establishing a trend difficult. The same results are presented in Figure 8 with the round-off error reduced by use of the graphically obtained derivative. The combination of finite difference and round-off error can almost completely obscure an experimental trend.

A combination of the various errors discussed in this and the preceding sections can result in an incorrect interpretation of experimental data. An example of the combined effect of round-off error and improper cleaning technique is shown in Figure 9. The rate of erosion presented as a function of the incremental weight of erodent follows a repeating pattern of a large weight loss followed by a small weight loss.

The result of an identical experiment conducted with ultrasonic cleaning of the specimen between erodent blasts is presented in Figure 10. A fairly smooth curve results with slight irregularities at the onset of erosion occurring within the limit of round-off error. The same data is presented in Figure 11 as shown in Figure 10. The sample was ultra-sonically cleaned, and the round-off error has been minimized by use of the graphical method of obtaining the erosion rate derivative. The oscillation is completely eliminated by use of ultrasonic-cleaning techniques and numerical differentiation.

5. Conclusions

Cutting is the preferred method for sizing specimens subject to gravimetric analysis. Surface preparation allows erosion to begin on a surface that is characteristic of the bulk material. The degree of surface preparation that is required is dependent upon the erosive character of the test.

Guidelines have been presented.

Accurate measurement of the solid particle velocity is needed to determine the effect of velocity on the erosion rate. A velocity measurement method based on time-series analysis is proposed.

The method of cleaning samples between weighings in successive blasting experiments can greatly influence the measured erosion rate. Ultrasonic cleaning in alcohol is recommended.

Round-off and finite difference errors can mask erosion rate data. A data analysis method has been presented which minimizes these errors.

References

1 I. Finnie, "Erosion of Surfaces by Solid Particles," *Wear, 3* (1960) 87.

2 J. Bitter, "A Study of Erosion Phenomena: Part I," *Wear, 6* (1963) 5.

3 J. Bitter, "A Study of Erosion Phenomena: Part II," *Wear, 6* (1963) 169.

4 G. P. Tilly, "Erosion Caused by Airborne Particles," *Wear, 14* (1969) 63.

5 I. Hutchings and R. R. Winter, "Particle Erosion of Ductile Metals: A Mechanism of Material Removal," *Wear, 27* (1974) 121.

6 Gunter Petzow, *Metallographic Etching,* American Society for Metals, 1978, p. 8.

7 Robert E. Reed-Hill, *Physical Metallurgy Principles,* 2nd edition, 1973, p. 2.

8 G. Sheldon, *Erosion of Brittle Materials,* Ph.D. Thesis, University of California, Berkeley, California, 1965.

9 T. Bakker, "Conducting Erosion Experiments Using the Room Temperature Tester," unpublished report, 1980.

10 V. Pannaganti, D. E. Stock and G. L. Sheldon, "Measurement of Particle Velocities in Erosion Processes," *ASME Symposium on Polyphase Flow and Transportation Technology, Proceedings of the Emerging Technology Conference,* San Francisco, August 13-15, 1980, ASME, New York, 1980, p. 217-222.

11 A. W. Ruff and L. K. Ives, "The Measurement of Solid Particle Velocity in Erosive Wear," *Wear, 35* (1975), 195.

12 K. T. Oki, T. Akehata, and T. Shirai, "A method For Measuring the Velocity of Solid Particles with Fiber Optic Probe," *Kagaku Kogaku, 37* (1973), 965.

13 M. S. Beck, J. Prane, A. Plokowski, and N Wainwright, "Particle Velocity and Mass Flow Measurement in Pneumatic Conveyors," *Powder Technology, 2* (1968/69), 269.

14 J. Werther and O. Molerus, "The Local Structure of Gas Fluidized Beds— I. A Statistically Based Measuring System," *International Journal of Multiphase Flow, 1* (1973), 103.

15 O. C. Jones, Jr. and Jean-Marc Delhaye, "Transient and Statistical Measurement Techniques for Two-Phase Flows: A Critical Review," *International Journal of Multiphase Flow, 3* (1976), 89.

16 D. M. Kleist, *One-Dimensional Two-Phase Particulate Flow,* M. S. thesis, University of California, Berkeley, 1977 (also known as Lawrence Berkeley Laboratory report LBL-6967).

17 Norman H. MacMillan, Pennsylvania State University, personal communication, January, 1982.

18 D. G. Rickerby and N. H. MacMillan, "The Erosion of Aluminum by Solid Particle Impingement at Normal Incidence," *Wear, 60* (1980), 369.

19 T. H. Kosel, A. P. L. Turner, R. O. Scattergood, "Effects of Particle Size and Shape on Erosive Wear Mechanisms," *Corrosion-Erosion Behavior of Materials Conference Proceedings of the Metallurgical Society of AIME,* St. Louis, Missouri, October 17-18, 1978, The Metallurgical Society of AIME, Warrendale, Pa., p. 146.

TABLE 1

Specimen Preparation Guidelines

Test	*Cutting*	*Grinding*	*Polishing*
Successive blasts (~300 gm total)	saw	320 grit	none
Single blast (~500 gm total)	saw	600 grit	none
Single particle (~10 particles)	shear or saw	600 grit	0.05 μm Alumina
SEM (cross section)	"Isomet" slow-speed saw	600 grit	0.05 μm Alumina

FIGURE CAPTIONS

Figure 1. Representation of a Metal Specimen; (a) Sized by Cutting and (b) Sized by Shearing.

Figure 2. Schematic Diagram of the Erosion Tester.

Figure 3. Erodent Particle Mass Flow Rate as a Function of Particle Mass Remaining in Hopper.

Figure 4. Schematic Diagram of the Erosion Tester with the Rotary-Disk Velocity Measurement Assembly in Place.

Figure 5. Optical Fiber Probe; (a) method of operation and (b) resulting signals.

Figure 6. Referenced Specimen Weight as a Function of Erodent Mass for 304 Stainless Steel with Method of Cleaning as a Parameter.

Figure 7. Erosion Rate as a Function of Erodent Mass for 310 Stainless Steel Calculated with the Finite-Difference Method and Using the Ultrasonic Cleaning Method.

Figure 8. Erosion Rate as a Function of Erodent Mass for 310 Stainless Steel Calculated with the Numerical-Derivative Method and Using the Ultrasonic Cleaning Method.

Figure 9. Erosion Rate as a Function of Erodent Mass for 304 Stainless Steel Calculated with the Finite-Difference Method and Using the Tissue Cleaning Method.

Figure 10. Erosion Rate as a Function of Erodent Mass for 304 Stainless Steel Calculated with the Finite-Difference Method and Using the Ultrasonic Cleaning Method.

Figure 11. Erosion Rate as a Function of Erodent Mass for 304 Stainless Steel Calculated with the Numerical-Derivative Method and Using the Ultrasonic Cleaning Method.

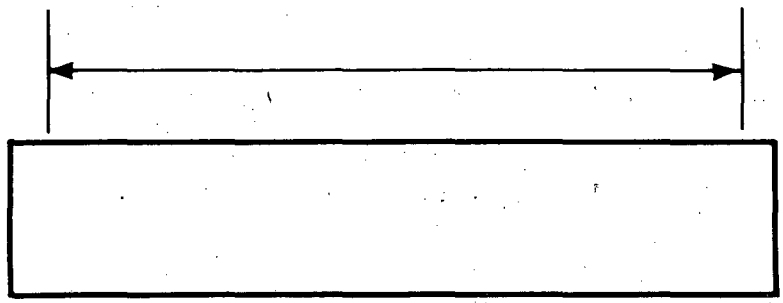

(a)

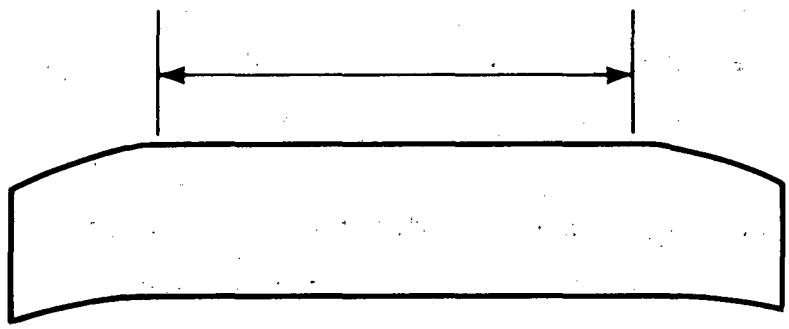

(b)

XBL 829-11714

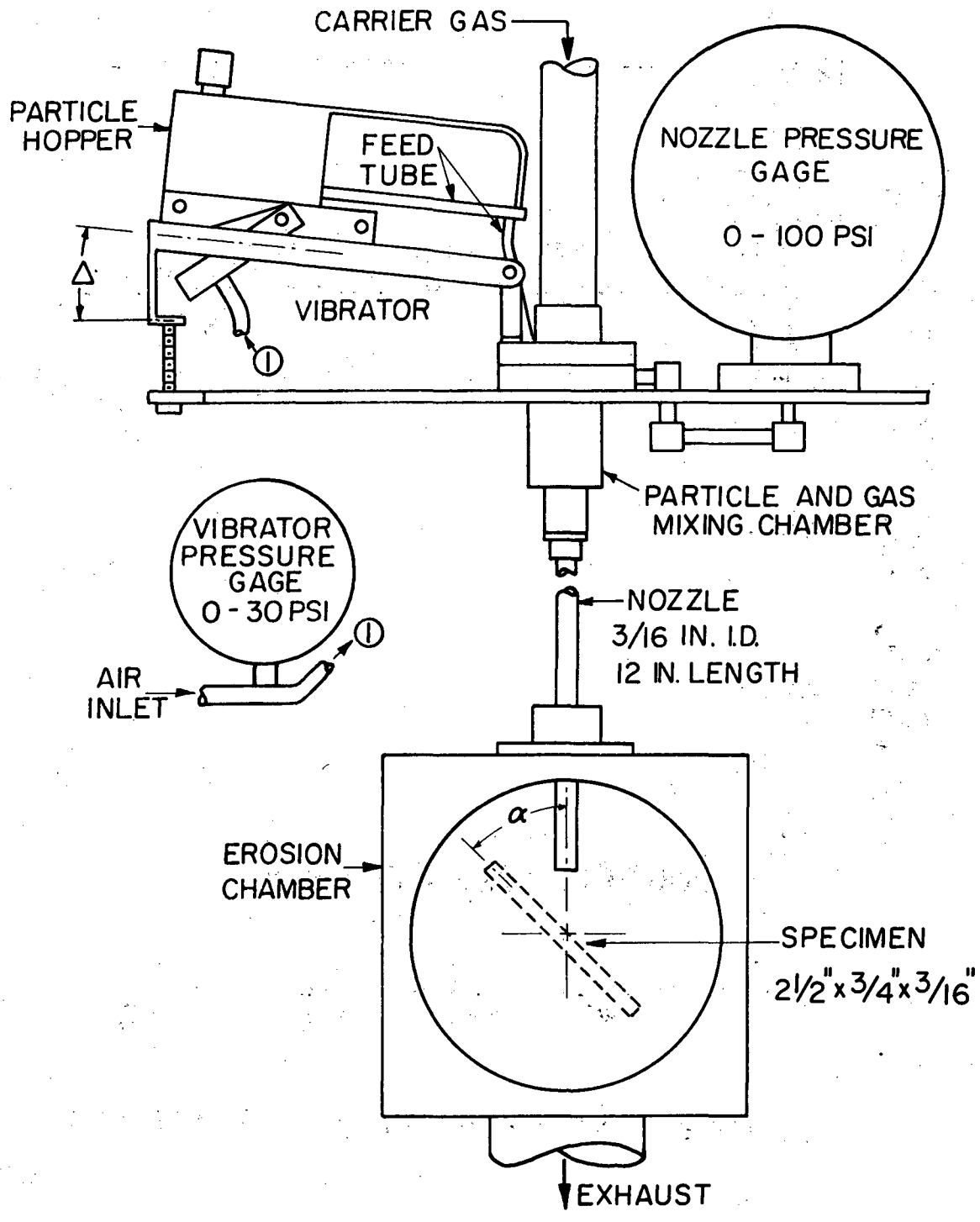
CARRIER GAS
PARTICLE HOPPER
FEED TUBE
NOZZLE PRESSURE GAGE
0 - 100 PSI
Δ
VIBRATOR
PARTICLE AND GAS MIXING CHAMBER
VIBRATOR PRESSURE GAGE
0 - 30 PSI
NOZZLE
3/16 IN. I.D.
12 IN. LENGTH
AIR INLET
α
EROSION CHAMBER
SPECIMEN
2½"x¾"x3/16"
EXHAUST

XBL775-5525

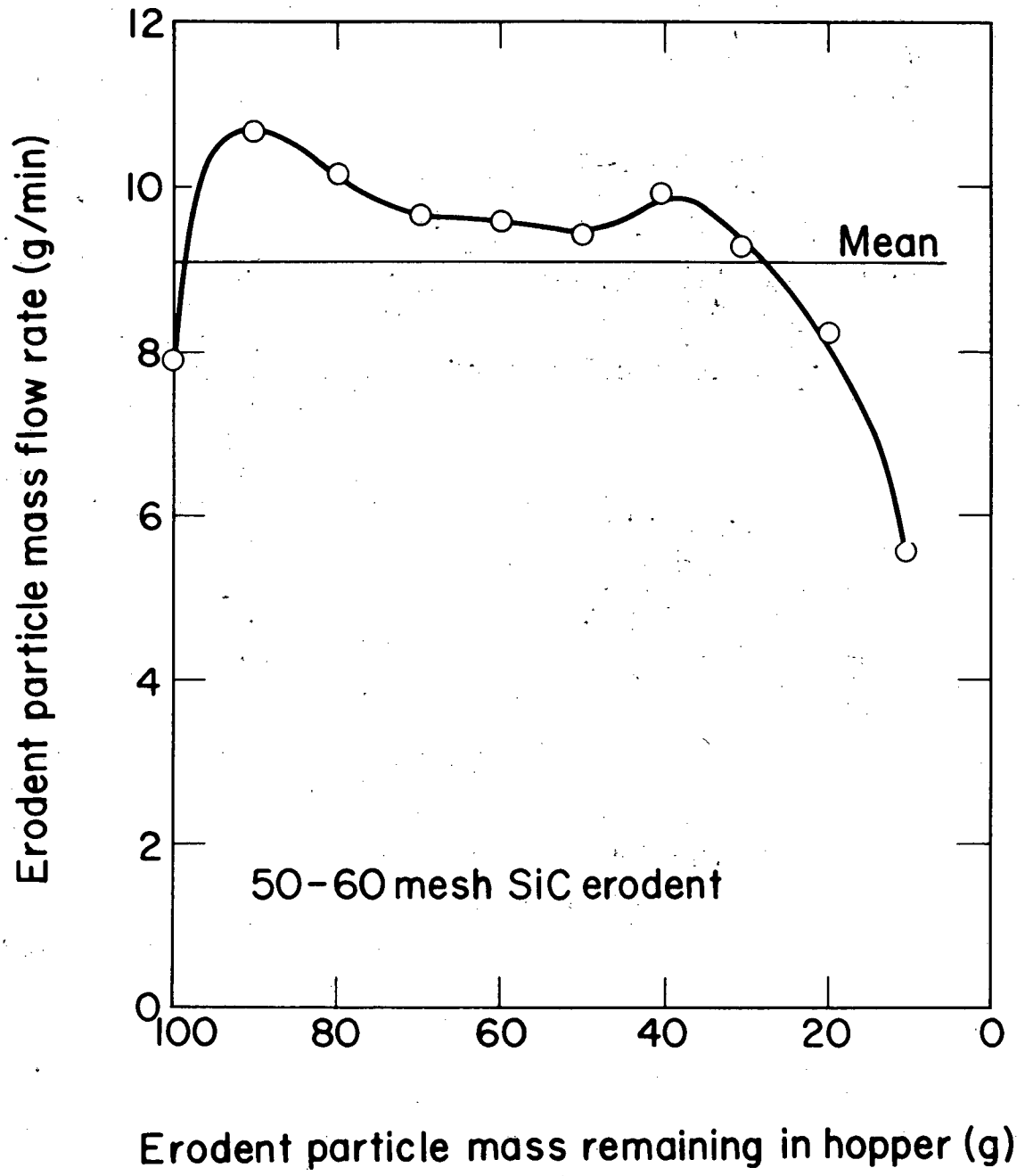
12
10
8
6
4
2
0
100
80
60
40
20
0
Mean
50-60 mesh SiC erodent
Erodent particle mass flow rate (g/min)
Erodent particle mass remaining in hopper (g)

XBL-827-7209

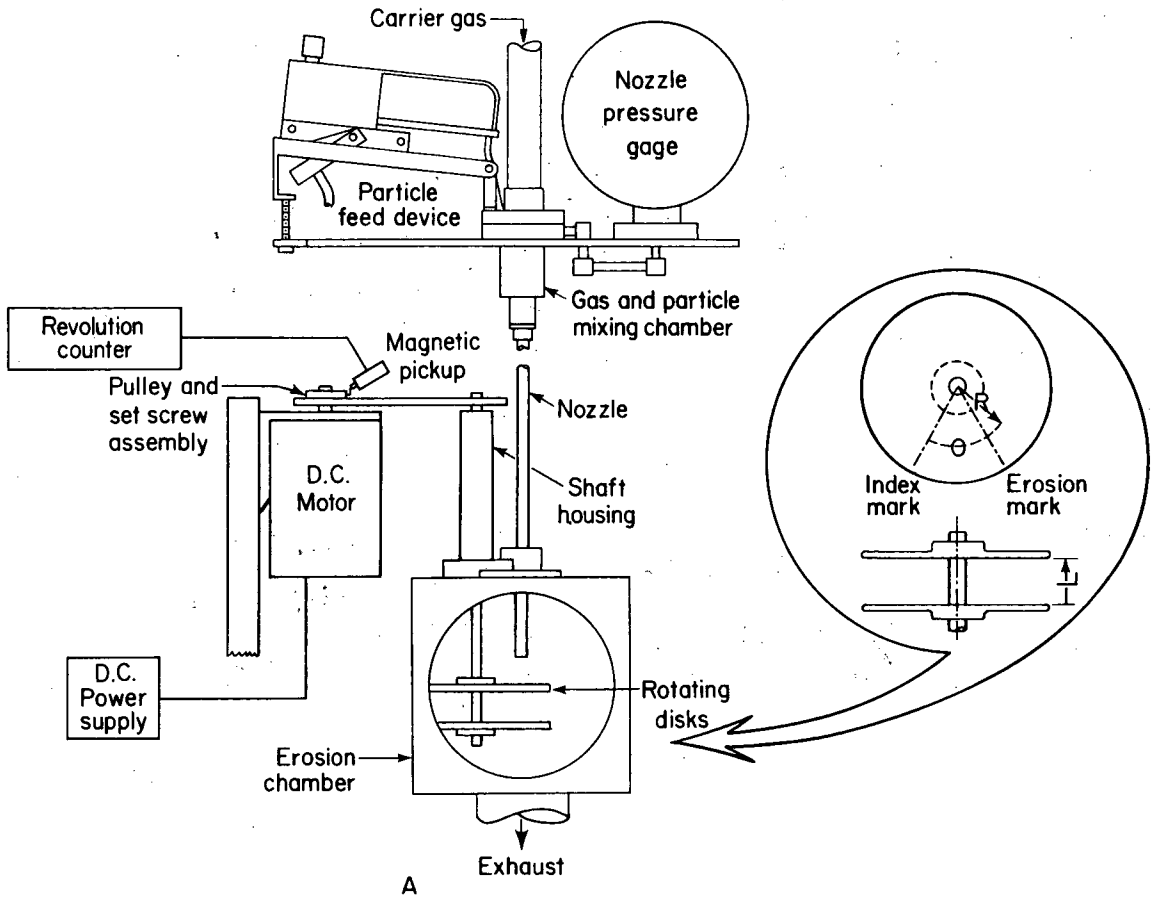

A

XBL-827-7212

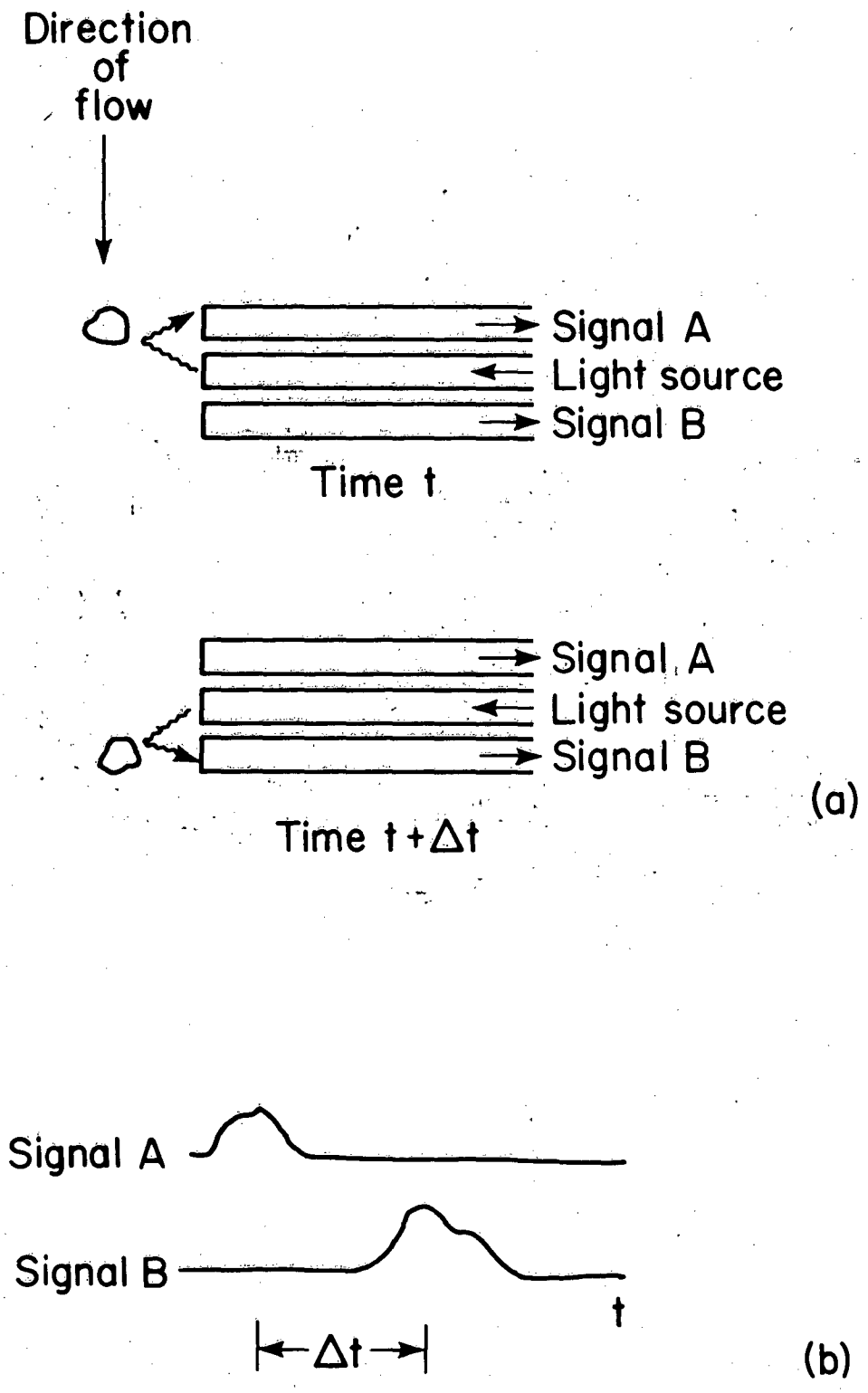
Direction of flow
Signal A
Light source
Signal B
Time t
Signal A
Light source
Signal B
Time t+Δt
(a)
Signal A
Signal B
t
Δt
(b)

XBL-827-7208

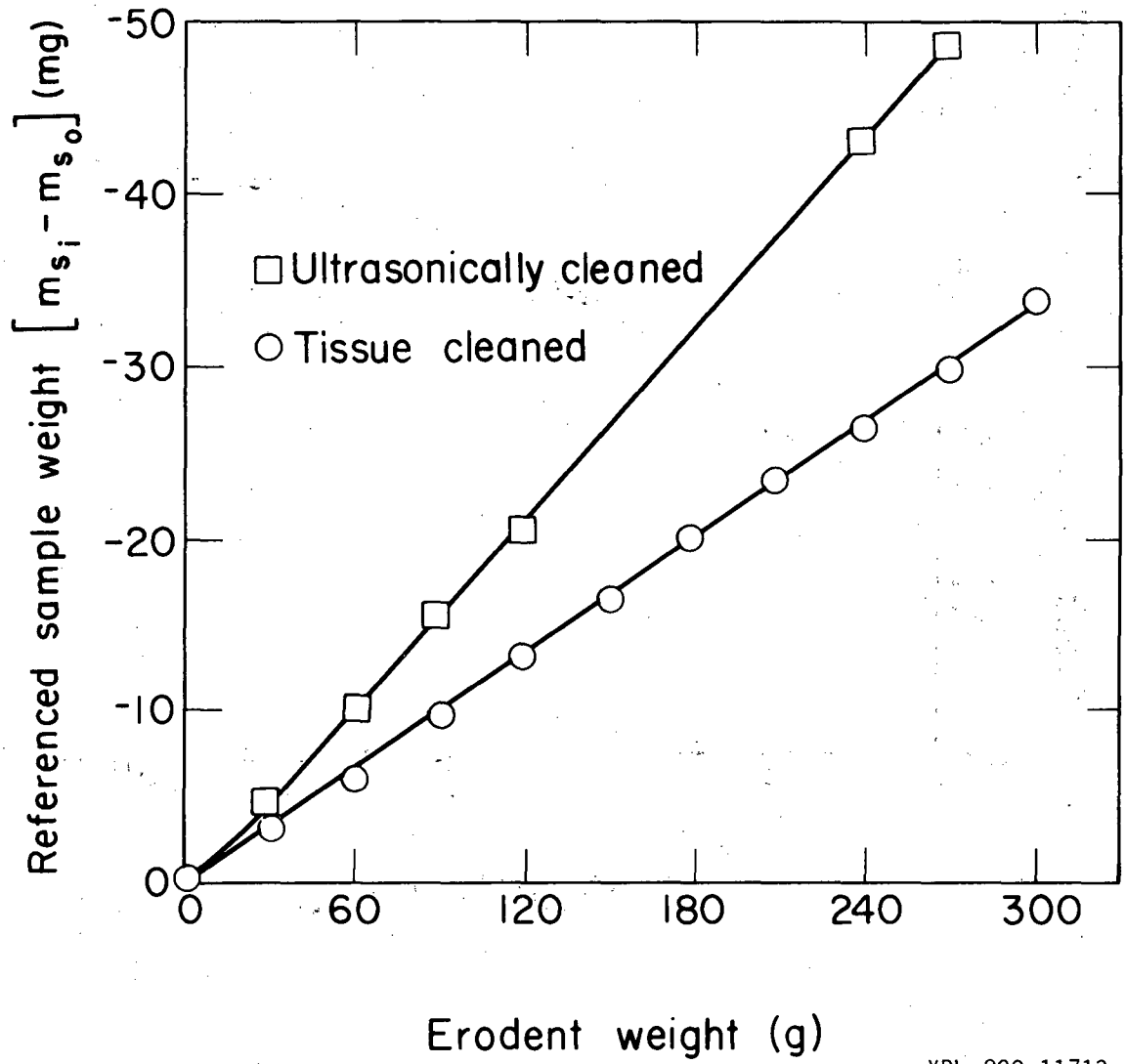

XBL 829-11713

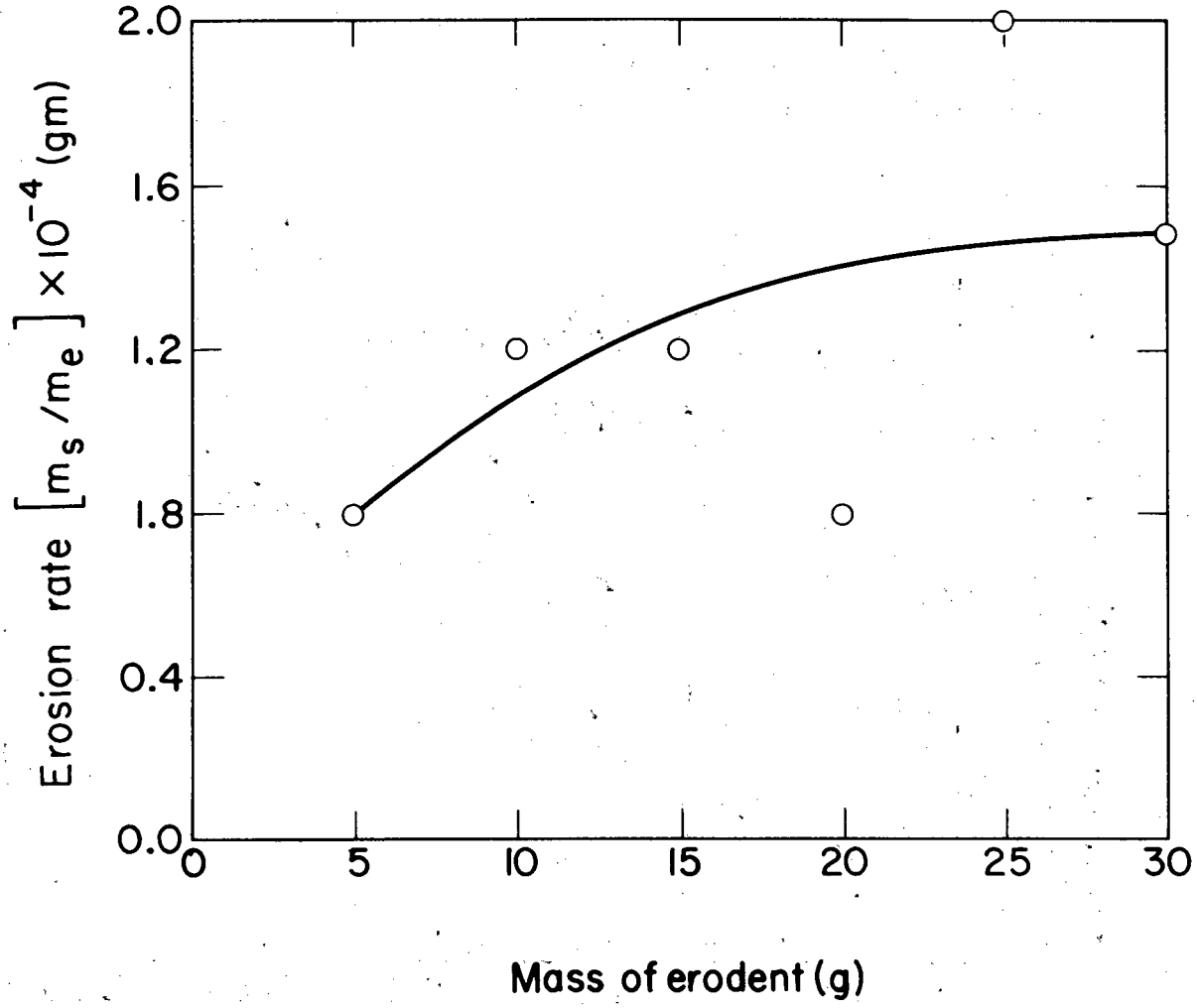
2.0
1.6
1.2
1.8
0.4
0.0
0
5
10
15
20
25
30
Erosion rate $[m_s/m_e] \times 10^{-4}$ (gm)
Mass of erodent (g)

XBL-827-7211

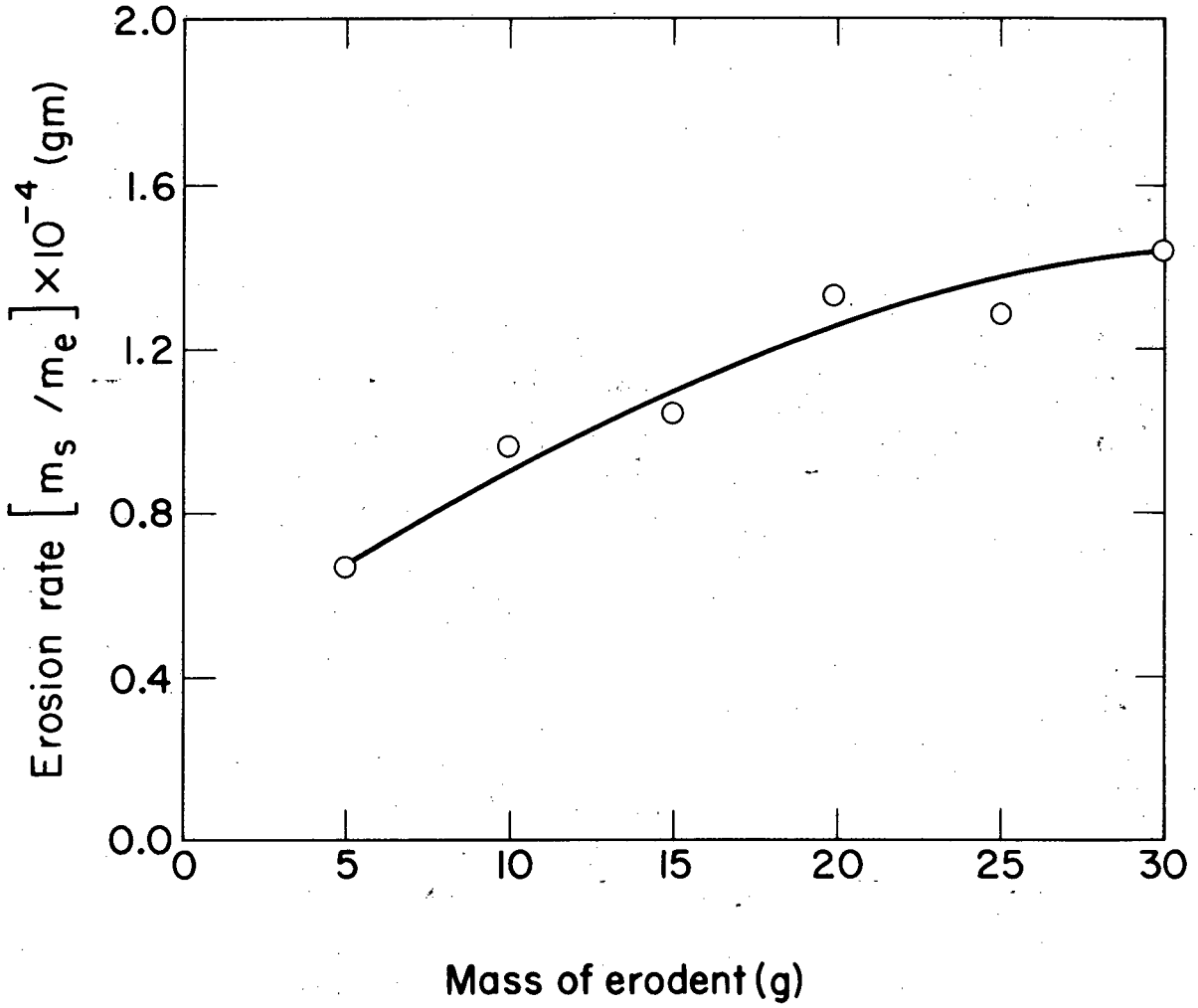
2.0
1.6
1.2
0.8
0.4
0.0
0
5
10
15
20
25
30
Erosion rate $[m_s / m_e] \times 10^{-4}$ (gm)
Mass of erodent (g)

XBL-827-7210

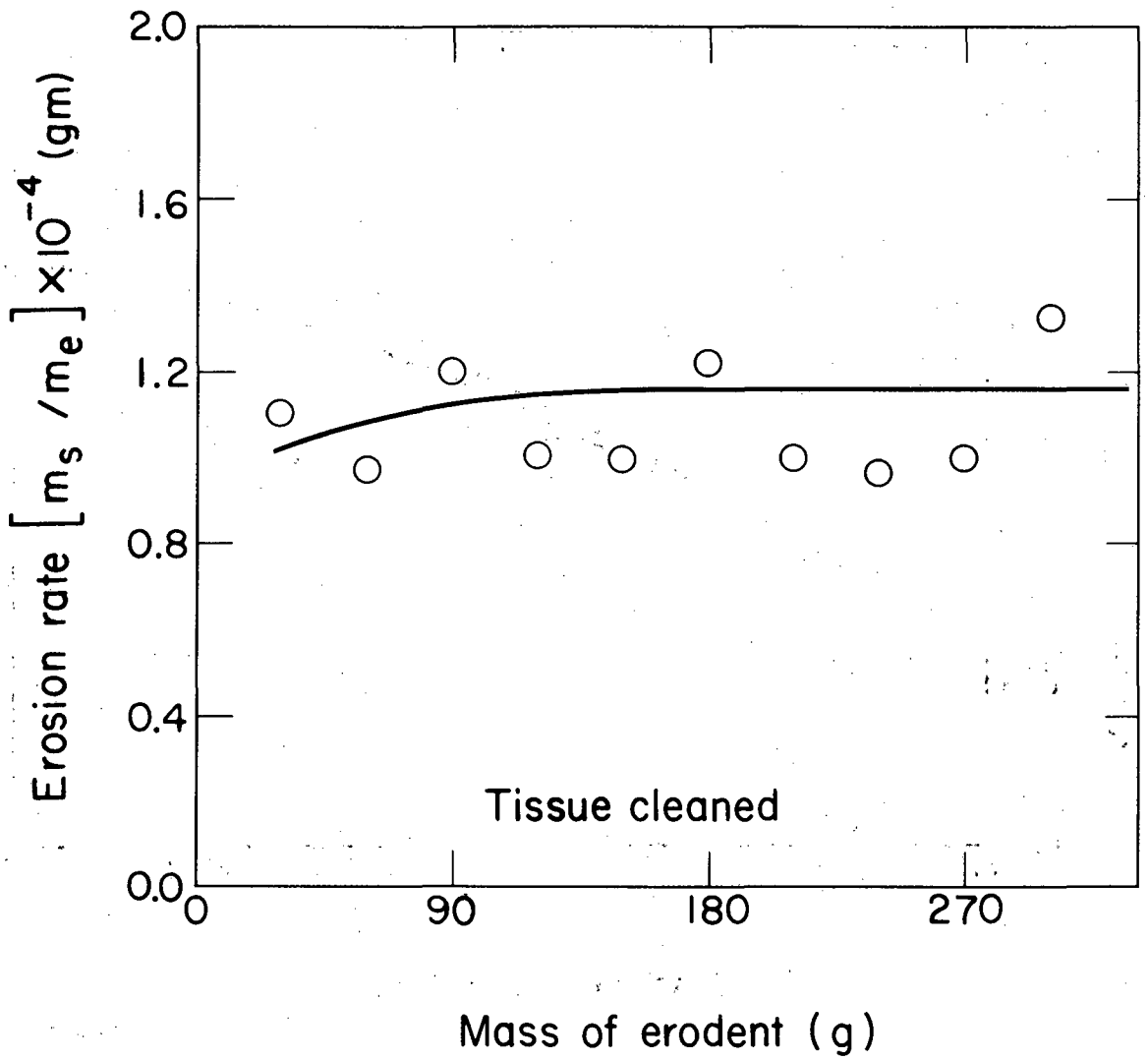
2.0
1.6
1.2
0.8
0.4
0.0
0
90
180
270
Erosion rate [m_s / m_e] x 10^{-4} (gm)
Tissue cleaned
Mass of erodent (g)

XBL-827-7214

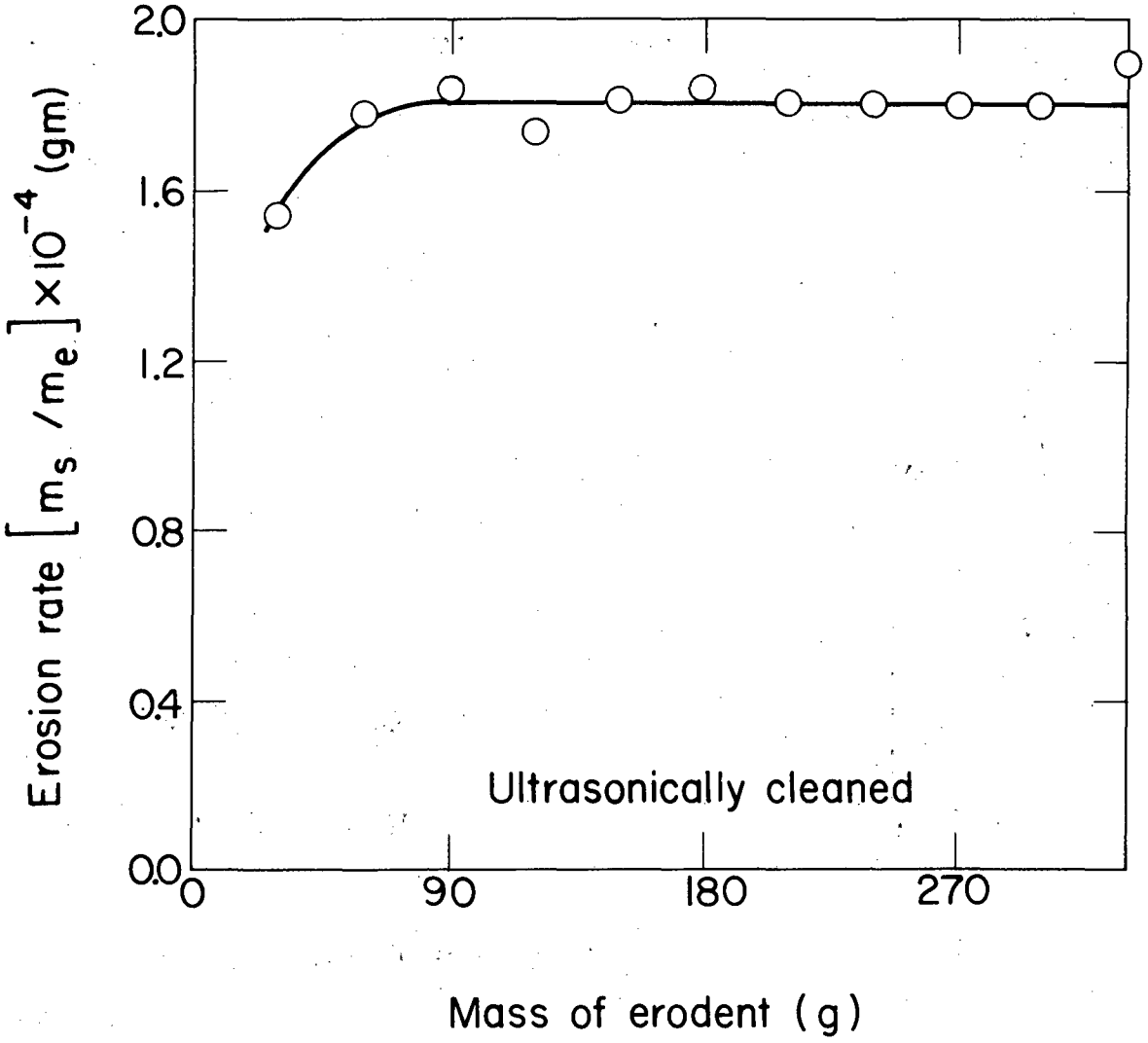
2.0
1.6
1.2
0.8
0.4
0.0
0
90
180
270
Erosion rate $[m_s/m_e] \times 10^{-4}$ (gm)
Ultrasonically cleaned
Mass of erodent (g)

XBL-827-7213

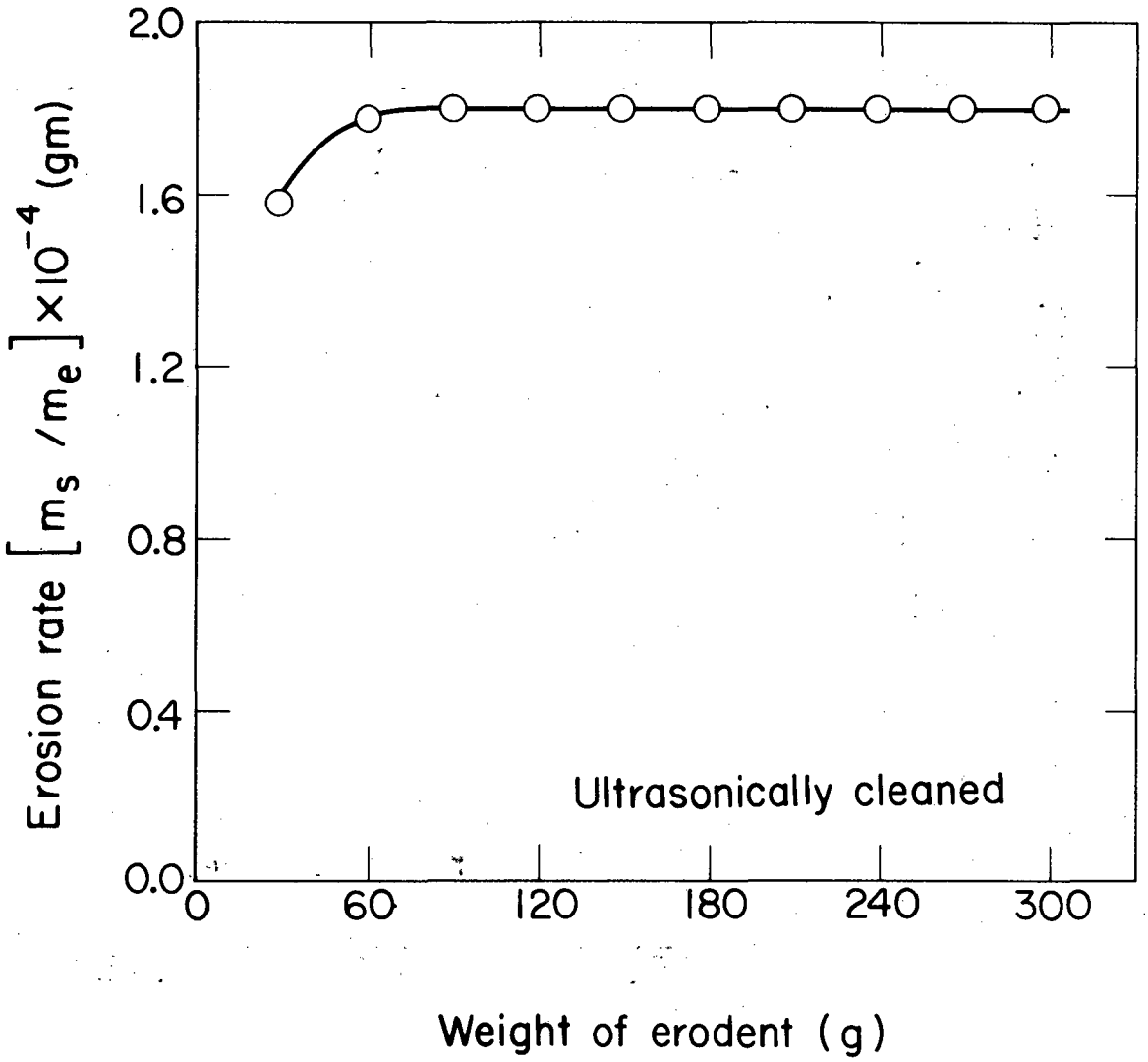
2.0
1.6
1.2
0.8
0.4
0.0
0
60
120
180
240
300
Erosion rate [m_s / m_e] $\times 10^{-4}$ (gm)
Ultrasonically cleaned
Weight of erodent (g)

XBL-827-7215

DISTRIBUTION LIST

Mr. R.A. Bradley, Manager
Fossil Energy Materials Program
Oak Ridge National Laboratory
P.O. Box X
Oak Ridge, TN 37830

Mr. S.J. Dapkunas
Department of Energy, Office of Fossil Energy
Technical Coordination Staff FE-14, Mailstop C-156 GTN
Washington D.C. 40525

Dr. P.T. Carlson, Task Leader
Fossil Energy Materials Program
Oak Ridge National Laboratory
P.O. Box X
Oak Ridge, TN 37830

Mr. E.E. Hoffman, Manager
National Materials Programs
Department of Energy
Oak Ridge Operations
P.O. Box E
Oak Ridge, TN 37830

Mr. J.M. Hobday
Department of Energy
Morgantown Energy Technology Center
P.O. Box 880
Morgantown, WV 26505

Mr. J.P. Carr
Department of Energy, Office of Fossil Energy
FE-42, Mailstop 3222-GTN
Washington D.C. 40525

DOE Technical Information Center
P.O. Box 62
Oak Ridge, TN 37830

Dr. R.R. Judkins
Fossil Energy Materials Program
Oak Ridge National Laboratory
P.O. Box X
Oak Ridge, TN 37830

Mr. E.L. Long, Jr.
Fossil Energy Materials Program
Oak Ridge National Laboratory
P.O. Box X
Oak Ridge, TN 37830

Edward Vesely
IITRI
10 West 35th St.
Chicago, IL 60616

Paul Shewmon
Dept. of Metallurgical Engineering
116 W. 19th Ave.
Columbus, OH 43210

Norman H. MacMillan
Pennsylvania State University
167 Materials Research Laboratory
University Park, PA 16802

Richard Brown
Materials Durability Division
College of Engineering
University of Delaware
Newark, DE 19711

Thomas Kosel
University of Notre Dame
Dept. of Metallurgical Engineering & Materials Science
Box E
Notre Dame, IN 46556

Gordon Sargent
University of Notre Dame
Dept. of Metallurgical Engineering & Materials Science
Box E
Notre Dame, IN 46556

Alberto Sagüés
IMMR — University of Kentucky
763 Anderson Hall
Lexington, KY 40506

Hans Conrad
Dept. of Materials Engineering
School of Engineering
North Carolina State University
PO Box 5427
Raleigh, NC 27650

Wate Bakker
EPRI
Hillview Ave.
Palo Alto, CA 94303

Susan M. Benford
NASA Lewis Research Center
21000 Brookpark Rd.
Cleveland, OH 41135

Mary Ellen Gulden
Solar Turbines International
PO Box 80966
San Diego, CA 92138

Ken Magee
Bingham-Willamette Co.
2800 N.W. Front Ave.
Portland, OR 97219

Sven Jansson
Stal-Laval Turbin AB
Finspong S-61220
Sweden

J.C. Williams
Dept. of Metallurgy & Materials Science
Carnegie-Mellon University
Schenley Park
Pittsburgh, PA 15213

Fred Pettitt
Dept. of Metallurgy and Materials Engineering
University of Pittsburgh
Pittsburgh, PA 15261

Ian Wright
Materials Science Division
505 King Ave.
Colombus, OH 43201

Bill Ellingson
9700 South Cass Ave.
Argonne, IL 60439

Widen Tabakoff
Dept. of Aerospace Engineering
University of Cincinnati
Cincinnati, OH 45221

This report was done with support from the Department of Energy. Any conclusions or opinions expressed in this report represent solely those of the author(s) and not necessarily those of The Regents of the University of California, the Lawrence Berkeley Laboratory or the Department of Energy.

Reference to a company or product name does not imply approval or recommendation of the product by the University of California or the U.S. Department of Energy to the exclusion of others that may be suitable.

TECHNICAL INFORMATION DEPARTMENT
LAWRENCE BERKELEY LABORATORY
UNIVERSITY OF CALIFORNIA
BERKELEY, CALIFORNIA 94720